



Cite this: *RSC Adv.*, 2020, **10**, 23245

An aluminium fluorosensor for the early detection of micro-level alcoholate corrosion[†]

Snigdha Roy,^a Sanju Das,^{ab} Rini Majumder,^a Ambarish Ray^{‡*b} and Partha Pratim Parui^{id}^{a*}

The detection of the dry alcoholate corrosion of aluminium is vital to design a corrosion resistive aluminium alloy for the storage and transportation of biofuel (methanol or ethanol). By synthesizing an Al^{3+} fluorescent probe operable in an alcoholic medium, we quantified the alcoholate corrosion in terms of the fluorometrically estimated soluble alkoxide ($\text{Al}(\text{OR})_3$) generation under nitrogen atmosphere. With time, a linear increase in corrosion with specific aluminium dissolution rate constants ~ 2.0 and $0.9 \mu\text{g}$ per day per cm^2 were estimated for aluminium and Al-7075 alloy, respectively. During open atmosphere monitoring, the adsorbed moisture converted small extent of $\text{Al}(\text{OR})_3$ to the insoluble $\text{Al}(\text{OH})_3$ at the alloy surface which retarded the alcoholate corrosion appreciably.

Received 20th January 2020
 Accepted 1st June 2020

DOI: 10.1039/d0ra00619j
rsc.li/rsc-advances

Switching over from conventional fossil fuel to biofuel is of current interest owing to the maximum utilization of eco-friendly non-conventional energy.¹ Commercially produced less polluted biofuels such as methanol and ethanol, mixed with fossil fuels have an acceptable performance capacity for the gasoline engine.² Moreover, in comparison to the gasoline, methanol and ethanol have much higher octane rating or compression ratio to resist the knocking for better thermal efficiency.³ Since most of the fuel tanks/pipes are made of aluminium or its alloys owing to its high strength-to-density ratio, the aluminium corrosion due to the formation of alkoxide (alcoholate or dry corrosion) during storage or even transportation of such bio-alcohols may cause leakage in the fuel tanks and in worst cases enough threat is speculated for fire and explosion.⁴ Mechanical overloads, alloy impurities even at elevated temperatures are further contenders for accelerating the alcoholate corrosion.⁵ However, a prolong exposure to the moisture retards the alcoholate corrosion by forming a protective layer of hydrated aluminium oxide in the metallic surface but moisture impurity in the fuel may damage the gasoline engine.⁶ Hence, a maintenance optimization is crucial in critical engineering disasters by detecting alcoholate corrosion as in its nascent state with minimizing the chance of water contamination.^{6,7}

Several electrochemical and mechanical methods have been exploited for decades to propose aluminium alcoholate and

other corrossions,⁶ yet the early detection of the alcoholate corrosion is still a challenging task due to the lack of sensitive analytical methods.^{6,8} Here, the fluorescence technique may act as a better alternative owing to its simplicity and high sensitivity.⁹ Till date, a large number of fluorescent probes for Al^{3+} have been exploited in the biological or environmental domain,¹⁰ but has never focused on alcoholate corrosion studies. Based on this requirement, we synthesized a fluorescent probe, namely HMBDC ((6Z)-6-(2-hydroxy-3-(hydroxymethyl)-5-methylbenzylideneamine)-2*H*-chromen-2-one), to detect alcoholate corrosion with μg -level detection ability along with its retarding signature in the presence of moisture in a judicious way. Such novel method may lead to an early detection of alcoholate corrosion in a simpler way.

The non-fluorescent phenolic Schiff-base molecule containing a coumarin moiety (HMBDC) was prepared by condensing an equimolar mixture of 6-amino coumarin (6-ACO) and 2-hydroxy-3-(hydroxymethyl)-5-methylbenzaldehyde (HHMB) in dry ethanol (Scheme 1 and Fig. S1[†]) (c.f. ESI[†] for details). Among various organic solvents, the interaction of HMBDC with Al^{3+} was observed only in the alcoholic medium according to the UV-vis studies (Fig. S2[†]). In methanol, the absorption intensity at $\sim 353 \text{ nm}$ for HMBDC (5 μM) decreased gradually with the continuous addition of $\text{Al}(\text{NO}_3)_3$ until saturated at ~ 8 -equiv., giving rise to a new peak at $\sim 406 \text{ nm}$, where an isosbestic point at $\sim 384 \text{ nm}$ assures the formation of Al^{3+} /HMBDC complex (**1**) (Fig. 1A). Upon optimization of the complex formation affinity in various ethanol/methanol mixed media, highest reactivity with the lowest saturated Al^{3+} concentration (~ 5 equiv.) compared to that obtained in pure methanol was observed in a 4 : 1 methanol/ethanol-mixed medium (Fig. S3[†]). Most probably, more effective H-bonding interaction of the dimeric ethanol/methanol¹¹ with **1** induces greater complex (**1**) stability, although the complex

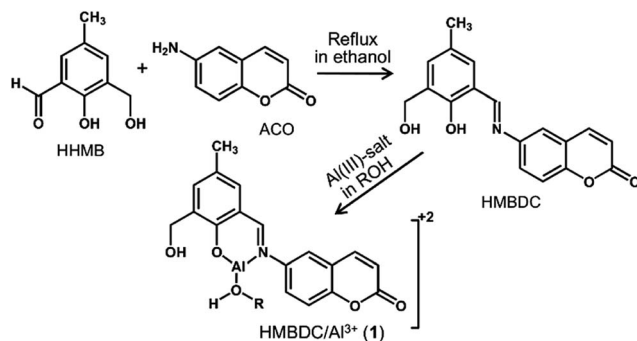
^aDepartment of Chemistry, Jadavpur University, Kolkata 700032, India. E-mail: parthaparui@yahoo.com; Fax: +91-33-24146223; Tel: +91-9433490492

^bDepartment of Chemistry, Maulana Azad College, Kolkata 700013, India. E-mail: r_ambarish@yahoo.co.in; Fax: +91-33-22268111; Tel: +91-9836650180

[†] Electronic supplementary information (ESI) available. See DOI: 10.1039/d0ra00619j

[‡] Department of Chemistry, Barasat Govt. College, Kolkata 700124, India





Scheme 1 Synthesis of HMBDC and its complexation with Al^{3+} in an alcohol solvent.

formation reactivity was much less in pure ethanol compared to the methanol medium (Fig. 1 and S2†).

In spite of the stronger H-bonding interactions of **1** with water compared to the methanol or ethanol, a complete dissociation of **1** in the presence of 20% (v/v) water in methanol (Fig. S4†) suggests that, in addition to the solvent assisted H-bonded structural stability of **1**, alcohol molecule may also participate in the coordination with Al^{3+} to form **1**. Indeed, the possible methanol coordination is reflected in the ESI-MS⁺ analysis (Fig. S5B†). In addition, the Job's plots in the absorption studies showed that the HMBDC formed 1 : 1 stoichiometric complex with Al^{3+} (Fig. S6†). To elucidate the probable structure of **1**, we carried out the DFT-based theoretical calculation by considering the 1 : 1 stoichiometric Al^{3+} /HMBDC

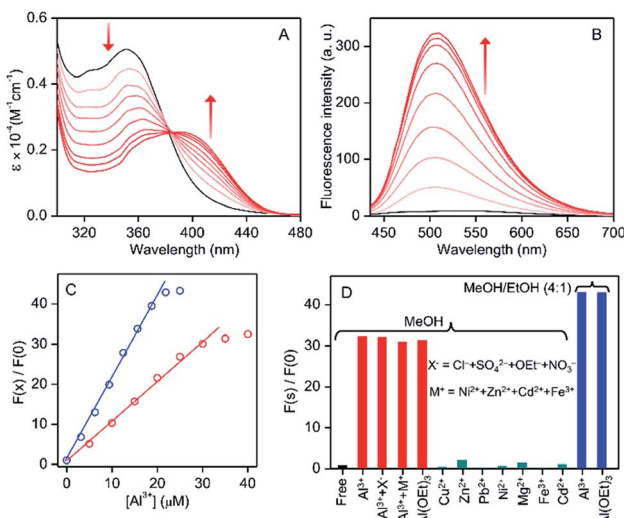


Fig. 1 (A) UV-vis absorption and (B) fluorescence spectra of HMBDC (5 μM) in the presence (red) and absence (black) of increasing concentration of $\text{Al}(\text{NO}_3)_3$ (0–40 μM) in anhydrous methanol at 25 °C. The intensity changes with increasing Al^{3+} concentrations are indicated by arrows. (C) Al^{3+} concentration dependent relative increase in the fluorescence intensity with respect to its absence in methanol (red) or methanol/ethanol (4 : 1) (blue). (D) Fluorescence intensity ratios in the presence and absence of various ions or mixture of ions in the mixed solvent (25 μM each; blue) or methanol (40 μM each; other colors) or are shown by bar-diagram.

complex with or without methanol coordination. A stable structure of **1** was obtained when the oxygen atom of the methanol molecule coordinates with Al^{3+} and other two coordination sites of Al^{3+} are occupied by the phenolic-oxygen and imine-nitrogen of HMBDC (Scheme 1, Fig. 2 and S7†). Facile coordination of those hard donor sites of HMBDC towards harder Al^{3+} is susceptible towards alcohol assisted stabilization of **1**. The UV-vis absorbance at ~ 402 nm for **1** computed from the time-dependent DFT (TD-DFT) calculations in methanol medium, where the HOMO (90) \rightarrow LUMO (92) excitation nicely matched with the experimental absorbance at ~ 406 nm (Fig. 1 and 2). However, monitoring of the $^1\text{H-NMR}$ peak characterized for aldimine proton is a useful strategy to identify the bonding of the imine-N to Al^{3+} .¹² We observed that the aldimine proton peak intensity for HMBDC in CD_3OD was quenched to a great extent with a considerable down-field shift from 8.80 to 8.88 ppm in the presence of Al^{3+} (Fig. S8†); the down-field shift is expected owing to the imine-N and Al^{3+} coordination, but intensity quenching does not follow the previous trend in the aprotic polar medium.¹² The generation of a partial positive charge at the N-centre upon its binding with the Al^{3+} may enhance the acidity of the aldimine proton to become labile for participating in the H/D exchange in a protic medium (CD_3OD), as reported previously for other allied systems.¹³ These results strongly suggest the imine-N and Al^{3+} bonding in **1**. On the other hand, Al^{3+} induced large decrease in the IR intensity at $\sim 3300 \text{ cm}^{-1}$ for phenolic-OH also supports the phenoxide coordination (Fig. S9†).

The electronic distribution in the molecular orbital diagram (MO) of the HMBDC evaluated from the DFT calculation showed an intra-molecular photo-induced electron transfer (PET) from coumarin to the HHMB moiety, which makes the HMBDC non-fluorescent (Fig. 2). Al^{3+} induced an instantaneous increase in the fluorescence intensity for HMBDC (5 μM) in the alcoholic medium (methanol/ethanol or their mixture) due to the formation of **1** (Fig. 1B and S10†). A gradual fluorescence intensity increase at ~ 506 nm ($\lambda_{\text{ex}} = 406$ nm) of ~ 30 -fold for 8 equiv. of

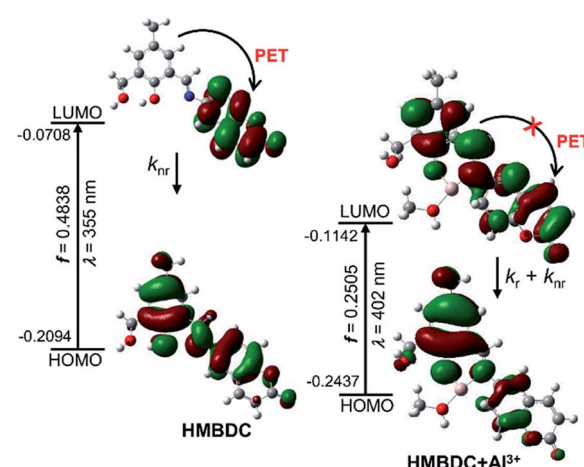


Fig. 2 Frontier molecular orbital profiles including various UV-vis absorption parameters of HMBDC (left panel) and HMBDC/ Al^{3+} complex (right panel) based on TD-DFT (B3LYP/6-31G(d)).



Al^{3+} and ~ 40 -fold for 5 equiv. of Al^{3+} was observed in the methanol and 4 : 1 (v/v) methanol/ethanol medium, respectively (Fig. 1 and S10B†). According to the HOMO and LUMO electronic distributions for **1** in the DFT studies, the PET process in HMBDC was highly restricted upon its binding with Al^{3+} in **1**, causing for the large increase in the fluorescence intensity (Fig. 2). However, the better fluorescence response (lower intensity-saturated Al^{3+} concentration and larger intensity increase) in the mixed medium than pure methanol may be associated with greater stability of **1**, as described in the previous section (Fig. S2†). The fluorescence intensity increase remains invariant using other soluble $\text{Al}(\text{m})$ -salts (Fig. 1D and S11†), which eliminates the role of counter anions for the increasing intensity. To ascertain the Al^{3+} selectivity, we performed similar fluorescence studies with other potentially interfering cations but failed to produce any noticeable fluorescence (Fig. 1D and S12†). However, a linear intensity increase with the increase in the concentration of Al^{3+} up to 6 equiv. in methanol and 4 equiv. in the 4 : 1 methanol/ethanol mixed medium can be useful for a ratiometric detection of unknown concentration of Al^{3+} (Fig. 1C), where the limit of detection¹⁴ (LOD) of Al^{3+} with HMBDC in the methanol medium was found to be $\sim 0.5 \mu\text{M}$ (c.f. details in ESI†). Most importantly, HMBDC recognized Al^{3+} selectively from the mixture of various other cations, and also in presence of other soluble $\text{Al}(\text{m})$ salts, particularly, aluminium alkoxide (ethoxide) with similar accuracy (Fig. 1D and S12†). Therefore, the $\text{Al}(\text{m})$ sensing ability for an alcoholate corrosion with an aluminium alloy must not be perturbed due to the interference of other leached cations.

The dry alcoholate corrosion of aluminium or its alloy while forming soluble alkoxide ($\text{Al}(\text{OR})_3$) can be detected upon incubation in an anhydrous alcoholic medium. However, under a condition of prolonged incubation, the contamination of trace amounts of moisture may also trigger the conversion of $\text{Al}(\text{OR})_3$ to $\text{Al}(\text{OH})_3$, followed by the hydrated alumina ($\text{Al}_2\text{O}_3 \cdot x\text{H}_2\text{O}$) coating on the metallic surface.⁶ The formation of hydrated alumina can also be possible *via* the decomposition of $\text{Al}(\text{OR})_3$.⁶ To characterize the alcoholate corrosion as an exclusive process to the maximum limit, we minimized those wet-processes by allowing the corrosion under inert conditions. A previously grazed aluminium-sheet (dimension $\sim 3.5 \times 1.5 \times 0.2 \text{ cm}^3$; surface area $\sim 12.5 \text{ cm}^2$) was incubated for 18 days in 100 mL anhydrous methanol or methanol/ethanol (4 : 1) mixed solvent under nitrogen atmosphere by purging nitrogen every 24 h, where the small change in the solution volume if required was adjusted by injecting an appropriate amount of the nitrogen-saturated anhydrous solvent. The amount of $\text{Al}(\text{OR})_3$ ($\text{R} = -\text{Me}, -\text{Et}$) generated in the medium was estimated by monitoring the HMBDC (5 μM) fluorescence. After 10-fold dilution of the medium with the parent solvent, the amount of $\text{Al}(\text{OR})_3$ formed or the alcoholate corrosion was estimated in every 3 days interval according to the amount of Al^{3+} obtained from the time-dependent fluorescence responses (Fig. S13†) as per the linear calibration plots in Fig. 1C multiplied by the dilution factor. A linear increase in the normalized fluorescence intensity from ~ 3.5 to 16.8 and ~ 7.3 to 36.1 was observed with an increase in the incubation time period from 3 day to 18 day for methanol and methanol/ethanol (4 : 1) media (Fig. 3A and S13†),

respectively, which correspond to the linear increase in the Al^{3+} amount in the medium from ~ 3.2 to 16.6 μmol for either solvents (Fig. 3C). Indeed, the weight-loss of $\sim 0.47 \text{ mg}$ *i.e.*, $\sim 17.5 \mu\text{mol}$ was found to be closely similar with that of the increase in Al^{3+} , revealing that not only the dry corrosion leads to the generation of Al^{3+} ($\text{Al}(\text{OR})_3$) as the only product, but also HMBDC is highly effective for an accurate estimation of the alcoholate corrosion. In addition, the nice correlation between the weight-loss and $\text{Al}(\text{OR})_3$ amount also reveals that the decomposition of alkoxide into insoluble alumina is negligibly small during the whole corrosion time-course.

However, under open atmospheric conditions maintained by air purging (average relative humidity $\sim 70\%$; average temperature 28 °C) in every 24 h interval while maintaining other similar experimental conditions and analysis protocol, the specific corrosion rate ($\sim 2.0 \mu\text{g}$ per day per cm^2) up to 12 days, was found to be closely similar to that detected under the nitrogen atmosphere (Fig. 3C and S13†). The results also indicate that the early stage of the alcoholate corrosion process (at least up to 12 days) for pure aluminium is not affected significantly by the atmospheric moisture content, although the final corrosion amount after 18 days incubation in normal atmosphere was slightly lower ($\sim 84\%$) for the mixed medium compared to that obtained for pure methanol (Fig. 3C). The decrease in the $\text{Al}(\text{OR})_3$ amount can be affected by two

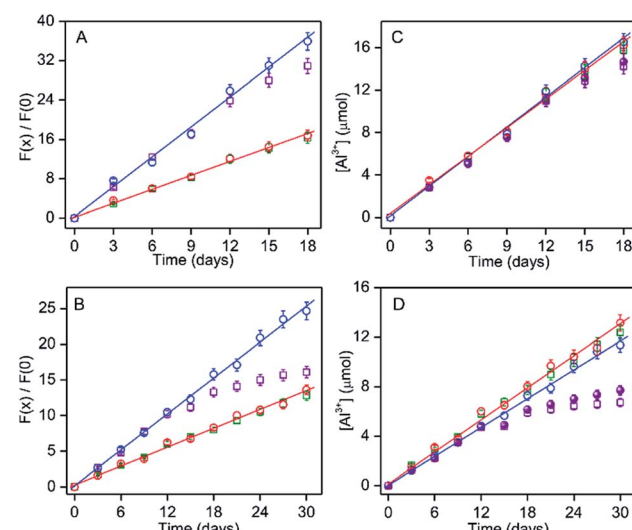


Fig. 3 (A and B) Extent of the fluorescence intensity increase due to corrosion-induced leached Al^{3+} ($F(x)/F(0)$) of HMBDC (5 μM) and (C and D) amount of Al^{3+} in the corrosion medium according to fluorescence response are plotted with various incubation times of pure aluminium sheet or its alloy (Al-7075) in different media/atmosphere conditions: nitrogen atmosphere in methanol (red) and methanol/ethanol (4 : 1) (blue); open atmosphere in methanol (green) and methanol/ethanol (4 : 1) (purple). The data at nitrogen conditions are only fitted linearly. (A and B) The fluorescence intensity of HMBDC (5 μM) were monitored after the 10-fold dilution of the corrosion medium with the same solvent. (C and D) The amount of Al^{3+} estimated as the amount obtained from the normalized intensity with comparing the linear plots in Fig. 1C multiplied by the dilution factor 10. The actual amount of alcoholate corrosion for the mixed medium under open atmosphere are depicted by solid circle (purple).



processes: (a) $\text{Al}(\text{OR})_3$ to insoluble $\text{Al}(\text{OH})_3$ conversion due to the adsorbed moisture; (b) actual retardation of the corrosion rate due to the surface deposition of $\text{Al}(\text{OH})_3$. The extent of the conversion of $\text{Al}(\text{OR})_3$ to $\text{Al}(\text{OH})_3$ in the corrosion medium under the open air condition can be assessed by estimating the fluorescence intensity at every 3 day time interval in the absence of aluminium sheet (from day-3 to day-18) with the addition of same amount of $\text{Al}(\text{OEt})_3$ (3.2, 5.7, 8.0, 11.7, 14.2 and 16.4 μmol (final added amount) at day 0 (beginning of day 1), 3, 9, 12 and 15, respectively, in 100 mL mixed medium) as that of the alkoxide amount detected due to the corrosion under nitrogen condition (Fig. S14†). In comparison to the actual added $\text{Al}(\text{OEt})_3$, any decrease in the $\text{Al}(\text{OEt})_3$ amount upon such incubation should be added with the corrosion induced formation of $\text{Al}(\text{OR})_3$ amount under nitrogen condition for respective time interval to obtain the actual alcoholate corrosion. The actual corrosion was found to be slightly higher than that estimated from the corrosion-induced $\text{Al}(\text{OR})_3$ formation (Fig. 3C, solid symbol). According to the LOD of Al^{3+} , the detection of the alcoholate corrosion amount as minimum as $\sim 0.1 \mu\text{g mL}^{-1}$ can be possible by monitoring the fluorescence response of HMBDC.

Alcoholate corrosion in a widely used aluminium alloy, Al-7075 (composition: Al, 90%; Zn, 5.5%; Mg, 2.5%; Cu, 1.5 and Si, 0.5%) was also studied. The previously grazed alloy sheet with same dimension and surface area as that of the pure aluminium sheet was incubated in 100 mL anhydrous methanol or 4 : 1 methanol/ethanol under nitrogen as well as normal atmospheric conditions. The amount of the alcoholate corrosion in every 3 days interval up to 30 days was estimated by evaluating the fluorescence response of HMBDC (Fig. 3B and S15†). In comparison to the pure aluminium sheet, the increase in corrosion from ~ 1.5 to $4.0 \mu\text{mol}$ evaluated from the increase in the normalized fluorescence intensity (1.65 to 5.90 in methanol; 2.64 to 10.40 in methanol/ethanol (4 : 1) mixture) with the increase in the incubation time from day-3 to day-12 follows a similar linear relation regardless of the solvent compositions and atmospheric conditions (Fig. 3B and D), while the intrinsic rate of corrosion $\sim 0.95 \mu\text{g per day per cm}^2$ was more than 2-fold slower (Fig. 3C and D). The lower rate constant value for the alloy compared to pure aluminium indicates that the contamination of other metals in the alloy resists the early stage alcoholate corrosion process. However, under normal atmospheric condition, the corrosion amount vs. time relation deviates from the linearity after 12 days. Importantly, after 30 days of incubation, a large reduction in the $\text{Al}(\text{OR})_3$ amount from ~ 11.38 to $6.64 \mu\text{mol}$ was estimated for the mixed medium, but the change was only from ~ 13.20 to $\sim 12.33 \mu\text{mol}$ for pure methanol (Fig. 3D). By determining the hydration-induced conversion amount of $\text{Al}(\text{OR})_3$ to $\text{Al}(\text{OH})_3$ according to the procedure, as described before (Fig. S16†), the actual alcoholate corrosion was found to decrease from ~ 11.38 to $7.70 \mu\text{mol}$ by changing the condition from nitrogen to open atmosphere after 30 days (Fig. 3D, solid symbol). Our study reveals that in comparison to pure methanol, the formation of $\text{Al}(\text{OH})_3$ under open atmospheric condition retards the alcoholate corrosion largely due to the presence of more hygroscopic ethanol.¹⁵ The deposition of $\text{Al}_2\text{O}_3 \cdot x\text{H}_2\text{O}$ onto the alloy-surface is responsible for resisting the further alcoholate corrosion⁶ (Fig. 3D).

In fact, the generation of more surface pits owing to the higher extent of the alcoholate corrosion in methanol over the mixed medium was also detected by naked eye (Fig. S17†). The surface morphology in the SEM studies showed that the alloy surface was little bit smoother after the corrosion in the mixed medium (Fig. S18†), justifying our proposition for the surface deposition of $\text{Al}_2\text{O}_3 \cdot x\text{H}_2\text{O}$. On the other hand, cyclic voltammetric studies in the corrosion medium exposed to normal atmospheric conditions identified an irreversible cathodic peak at $\sim -0.7 \text{ V}$ due to the formation of insoluble $\text{Al}(\text{OH})_3$ in addition to the conversion from Al to Al^{3+} , but such irreversible peak was not observed for the medium exposed to nitrogen (Fig. S19†). Moreover, the formation of white gelatinous precipitate of $\text{Al}(\text{OH})_3$ in the mixed medium was clearly visible by naked eye under normal atmospheric conditions (Fig. S17B†). All those results strongly support that the initiation of the wet-process by forming $\text{Al}(\text{OH})_3$ inhibits the alcoholate corrosion rate.

In conclusion, a phenolic Schiff-base consisting of a coumarin unit as a fluorescent sensor for Al^{3+} operable only in the alcoholic medium is synthesized to monitor dry alcoholate corrosion. The photo-induced electron transfer process in the probe molecule exhibits Al^{3+} induced large increase of fluorescence intensity, lifted by its complexation with Al^{3+} , which was further stabilized by the coordination and H-bonding interaction with the solvent molecule. The alcohol specific complex formation and subsequent fluorescence generation was suitably tuned to monitor the alcoholate corrosion by fluorometrically estimating aluminium alkoxide formation with a sensitivity of $\sim 10 \mu\text{g L}^{-1}$. However, the simultaneous participation of small extent of the wet-process ($\text{Al}(\text{OR})_3$ to $\text{Al}(\text{OH})_3$ conversion) and its deposition in metal surface, particularly for the alloy, inhibits the dry alcoholate corrosion. The alloy specific detection of the early stage alcoholate corrosion is in progress to obtain suitable material useful as a biofuel container.

Conflicts of interest

There are no conflicts to declare.

Acknowledgements

This study is partially supported by UGC and government of West Bengal for financial support under RUSA 2.0 scheme (PPP; No: 5400-F(Y)). SR and RM acknowledge UGC for the SRF fellowship. Authors also acknowledge JU and MA College, for departmental facilities. We are thankful to Dr N. R. Singha (GCELT) for TGA studies.

Notes and references

- (a) J. Xuan, D. Y. C. Leung, M. Ni and M. K. H. Leung, *Renew. Sustain. Energy Rev.*, 2009, **13**, 1301; (b) F. H. Shinya and Y. Kenjilimou, *Bioresour. Technol.*, 2010, **101**, 109.
- (a) L. Matejovsky, J. Macak, M. Pospisil, P. Baros, M. Stas and A. Krausova, *Energy Fuels*, 2017, **31**, 10880; (b) R. H. Borgwardt, *Ind. Eng. Chem. Res.*, 1998, **37**, 3760; (c) B. Shayan, S. M. Seyedpour, F. Ommi, S. H. Moosavy and



M. Alizadeh, *Int. J. Automot. Mech. Eng.*, 2011, **1**, 3; (d) J. H. Lunsford, *Catal. Today*, 2000, **63**, 165.

3 M. B. Çelik, B. Ozdalyan and F. Alkan, *Fuel*, 2011, **90**, 1591.

4 K. Wagner, K. Eppel, T. Troßmann and C. Berger, *Energy Mater. Mater. Sci. Eng. Energy Syst.*, 2008, **3**, 227.

5 K. Eppel, M. Scholz, T. Troßmann and C. Berger, *Proceedings: EUROCORR*, 2009, Nice, p. 9.

6 J. Linder, thesis on, Alcoholate corrosion of aluminium in ethanol blends, Master thesis, KTH Royal Institute of Technology, Div. Surface and Corrosion Science, Stockholm, 2012.

7 (a) P. B. L. Fregolente, M. R. Wolf Maciel and L. S. Oliveira, *Braz. J. Chem. Eng.*, 2015, **32**, 895; (b) S. K. Thangavelu, A. S. Ahmed and F. N. Ani, *Int. J. Energy Res.*, 2016, **40**, 1704.

8 (a) L. Kruger, F. Tuchscheerer, M. Mandel, S. Muller and S. Liebsch, *J. Mater. Sci.*, 2012, **47**, 2798; (b) O. Seri and Y. Kido, *Mater. Trans.*, 2009, **50**, 1433; (c) Corrosion resistance of aluminium and protective measures where appropriate, First Edition: 2011 © AFSA Compiled and published by the Aluminium Federation of South Africa; (d) G. R. Kramer, C. M. Mendez and A. E. Ares, *Mat. Res.*, 2018, **21**, 1.

9 (a) S. Das, Y. Sarkar, S. Mukherjee, J. Bandyopadhyay, S. Samanta, P. P. Parui and A. Ray, *Sens. Actuators, B*, 2015, **209**, 545; (b) P. P. Parui, A. Ray, S. Das, Y. Sarkar, T. Paul, S. Roy, R. Majumder and J. Bandyopadhyay, *New J. Chem.*, 2019, **43**, 3750; (c) P. A. Anna, P. Paul and W. R. David, *Anal. Chem.*, 1997, **69**, 1635.

10 (a) A. Gupta and N. Kumar, *RSC Adv.*, 2016, **6**, 106413; (b) Q. Jiang, M. Li, J. Song, Y. Yang, X. Xu, H. Xu and S. Wang, *RSC Adv.*, 2019, **9**, 10414; (c) H. L. Nguyen, N. Kumar, J.-F. Audibert, R. Ghesami, J.-P. Lefevre, M.-H. Ha-Thi, C. Mongin and I. Leray, *New J. Chem.*, 2019, **43**, 15302.

11 I. A. Finneran, P. B. Carroll, G. J. Mead and G. A. Blake, *Phys. Chem. Chem. Phys.*, 2016, **18**, 22565.

12 S. Sahana, S. Bose, S. K. Mukhopadhyay and P. K. Bharadwaj, *J. Lumin.*, 2016, **169**, 334.

13 (a) R. Casasnovas, M. Adrover, J. Ortega-Castro, J. Frau, J. Donoso and F. Muñoz, *J. Phys. Chem. B*, 2012, **116**, 10665; (b) B. Setner, M. Wierzbicka, L. Jerzykiewicz, M. Lisowski and Z. Szewczuk, *Org. Biomol. Chem.*, 2018, **16**, 825.

14 V. Thomsen, D. Schatzlein and D. Mercuro, *Spectroscopy*, 2003, **18**, 112.

15 B. Tan, P. Melius and P. Ziegler, *J. Chromatogr. Sci.*, 1982, **20**, 213.

